Highly Efficient Estimators with High Breakdown Point for Linear Models with Structured Covariance Matrices

Lopuhaä, Hendrik Paul

DOI
10.1016/j.ecosta.2023.03.003

Publication date
2023

Document Version
Final published version

Published in
Econometrics and Statistics

Reliability Engineering and System Safety 242 (2024) 109715

Contents lists available at ScienceDirect

Reliability Engineering and System Safety

journal homepage: www.elsevier.com/locate/ress

Uncertainty analysis and interval prediction of LEDs lifetimes

Roberto Rocchetta [a,*], Zhouzhao Zhan [a], Willem Dirk van Driel [b,c], Alessandro Di Bucchianico [a]

[a] Eindhoven University of Technology, Department of Mathematics and Computer Science, P.O. Box 513, Eindhoven, 5600 MB, The Netherlands
[b] Delft University of Technology, Department of Microelectronics, Mekelweg 5, Delft, 2628 CD, The Netherlands
[c] Signify, High Tech Campus 7, Eindhoven, 5656 AE, The Netherlands

ARTICLE INFO

Keywords:
Light-emitting Diodes
Lifetime
Lumen maintenance
Uncertainty Quantification
Accelerated Degradation Data
Interval Prediction

ABSTRACT

Lifetime analyses are crucial for ensuring the durability of new Light-emitting Diodes (LEDs) and uncertainty quantification (UQ) is necessary to quantify a lack of usable failure and degradation data. This work presents a new framework for predicting the lifetime of LEDs in terms of lumen maintenance, effectively quantifying the natural variability of lifetimes (aleatory) as well as the reducible uncertainty resulting from data scarcity (epistemic). Non-parametric survival models are employed for UQ of low-magnitude failures, while a new parametric interval prediction model (IPM) is introduced to characterize the uncertainty in high-magnitude lumen depreciation events and long-term extrapolated lifetimes. The width of interval-valued predictions reflects the inherent variability in degradation paths whilst the epistemic uncertainty, arising from data scarcity, is quantified by a statistical bound on the probability of the prediction errors for future degradation trajectories. A modified exponential flux decay model combined with the Arrhenius equation equips the IPM with physical information on the physics of LED luminous flux degradation. The framework is tested and validated on a novel database of LED degradation trajectories and in comparison to well-established probabilistic predictors. The results of this study support the validity of the proposed approach and the usefulness of the additional UQ capabilities.

1. Introduction

Producing durable and reliable light-emitting diodes (LEDs) has become paramount in the lighting industry leading to extensive efforts in understanding failure modes, degradation mechanisms, and reliability-related issues [1–3]. Among the most common failure mechanisms, degradation-related failures occur when LEDs no longer meet the desired functionality requirements, such as exceeding a maximum luminous flux depreciation. To gather usable data concerning luminous flux degradation and to better support lifetime assessment and reliability analyses, accelerated degradation tests (ADTs) are often employed [4,5]. The Illuminating Energy Society (IES) of North America has established dedicated standards, including LM-80, TM-21-11, and LM-84-14 [6,7], to guide practitioners in ADTs and the modeling of luminous flux degradation, and for lifetime predictions. Additionally, various degradation indicators, such as those proposed in ANSI/IES TM-35 [8–10], have been suggested in the literature.

Accurate and robust LED lifetime predictions require the careful quantification of aleatory uncertainty (irreducible and due randomness and natural variability) and also epistemic uncertainty, which arises from a lack of data and model imprecision [11], which can be in principle reduced [12,13]. Aleatory uncertainty has been extensively studied in LED lifetime analyses, with a significant focus on the heterogeneity of the LED population [14], random measurement errors and variability in mission profiles [15]. Numerous studies focused on assessing the limitations of the standard TM-21 and have aimed to enhance lifetime predictions by improving the characterization of the randomness in lumen depreciation trajectories. In this respect, data-driven [16], physics-based [17], and hybrid [18,19] Prognostics and Health Management (PHM) frameworks have been proposed to better characterize stochastic errors in the LED lifetime distributions. Probabilistic and machine learning (ML) approaches to model degradation trajectories have been recently reviewed by [20] and Wiener–Levy [21–24], Gamma [25], and Gaussian processes [26,27] identified as the most widely applied concepts. In [28], a Bayesian model has been proposed to identify luminaires with early degradation onset while filter-based algorithms have been applied to predict LED lifetimes, e.g., [29,30]. However, only a few studies have explicitly quantified the epistemic uncertainty arising from a limited number of degradation

* Corresponding author.
E-mail address: roberto.rocchetta@supsi.ch (R. Rocchetta).

https://doi.org/10.1016/j.ress.2023.109715
Received 11 October 2022; Received in revised form 27 June 2023; Accepted 6 October 2023
Available online 26 October 2023

trajectories, censored lifetime data, and model uncertainty, e.g., [26,27,31–33]. Specifically, [26,27] analyzed correlations between degradation patterns and missing data issues and [33] analyzed both natural variability and epistemic uncertainty lifetime dynamic via a semi-analytical approach. None of the revised works proposed a framework for interval prediction of LED lifetime and for a formal quantification of both aleatory and epistemic uncertainties.

To address the identified gap in the existing literature, this paper introduces a new framework for LED lumen maintenance life predictions and uncertainty quantification. A new database with LED degradation data is also introduced for testing and validating the novel approach. Within the framework, non-parametric Kaplan–Meier estimators and Probability boxes (P-boxes) characterize the epistemic and aleatory uncertainty associated with low-magnitude degradation events. These models are driven uniquely by (censored) lifetime data and are only applicable to low-magnitude depreciation events. On the other hand, high-magnitude depreciation events and lifetimes predictions require parametric model assumptions for long-term extrapolation of the degradation paths. In this work, a new Interval Predictor Model (IPM) is proposed to predict the LED lifetime and incorporates a modified exponential decay model and thermo-electrical ageing to account for the physics of the problem. The interval predictions from the IPM establish lower and upper bounds for lumen degradation trajectories, i.e., a non-probabilistic interval-valued quantification of the inherent variability affecting lumen degradation trajectories and the lifetimes. To evaluate the robustness of the IPM model, a formal bound on the IPM's probability of error is proposed, that is, a non-asymptotic and distribution-free statistical bound which holds independently of assumptions regarding error distribution and for any number of samples. Importantly, it quantifies the epistemic uncertainty arising from a limited number of degradation trajectories. The framework is tested and validated on the dataset of the new degradation data and the lifetime predicted by the IPM compared with those predicted by a well-established random coefficient regression model [34,35] and the TM-21 standard [6,7]. The outcomes of the analysis confirm the high durability of the selected LED packages while confirming a valid lifetime bound prescribed by the IPM model, i.e., compatible with the results of the random coefficient model. In addition to this result, the statistical error bounds for the IPM ensure a minimum reliability level for the IPM model and an upper bound on the error probability for out-of-sample depreciation trajectories. This result highlights that significant epistemic uncertainty remains in long-term lumen maintenance predictions. The main contributions of this work can be summarized as follows:

- A new database for LED durability analysis comprising accelerated degradation data from several LEDs.
- A new framework for LED lifetimes analysis and UQ based on non-parametric P-boxes and parametric physics-informed IPMs.
- Statistical bounds are computed and quantify the epistemic uncertainty associated with the IPM (arising from a lack of data and model over-complexity).

2. Reliability and degradation models for LEDs

LED failures are of two main types, (1) degradation-related and (2) catastrophic. The former relates to progressive losses in functionality exceeding unacceptable threshold levels. Catastrophic failures follow a sudden and total loss of functionality, e.g., a sudden loss of light due to electrical over-stress [3]. This work will only focus on degradation-induced failures. A summary of reliability performance requirements for LEDs, accelerated degradation data, and well-established degradation models is presented next.

2.1. Reliability requirements

LED lifetimes associated with degradation events are determined based on the first passage of predefined thresholds that indicate inadmissible degradation of reliability performance indicators, e.g., luminous flux, $\phi(t)$, or chromatic shift, $\Delta u'v'$. The lifetime L_p defines the point at which a percentage $1-p$ of the initial performance is lost and, for luminous flux, $p \in [0,1]$ determines a threshold lumen maintenance, a minimum acceptable light output rating. A higher value of p indicates a stricter lifetime requirement and its selection is application-dependent, e.g., up to 30% for indoor applications and only 10% depreciation for street lighting. The corresponding lifetime, $L_{0.70}$ and $L_{0.9}$, define operating times for which the luminous flux drops below 70% and 90% of the initial flux value, respectively. Other degradation indicators can be investigated, see e.g., [1,2,9,10], however, this work will focus on lifetime defined by lumen maintenance.

2.2. Accelerated flux degradation data

Flux degradation data collected from a constant-stress accelerated experiments, e.g., LM-80, define the following dataset:

$$\mathcal{D} = \left\{ \{\boldsymbol{\phi}_{a,k}\}_{k=1}^{n_s}, T_a, I_a \right\}_{a=1}^{n_a}, \tag{1}$$

where $\boldsymbol{\phi}_{a,k} = \{\phi_{a,k,\tau}\}_{\tau=1}^{n_t}$ are luminous flux degradation trajectories collected from $k = 1,\dots,n_s$ identical LEDs under the accelerated temperature T_a and forward current I_a and n_a, n_t are the number of stressors combinations and flux measurements for each LED, respectively. Catastrophic failures that involve a fast and significant decrease in lumen maintenance, e.g., from values larger than 90% to lower than 60% in a month, are not considered in this work and thus removed from $\mathcal{D}$. In practice, the values of n_s and n_t vary depending on the specific conditions, such as the sampling frequency and the number of LEDs tested. These values may be higher for certain acceleration levels, however, to simplify the presentation, this dependency has been omitted in the notation.

2.3. Lifetime and lumen maintenance

The lifetime L_p corresponding to a minimum acceptable lumen maintenance p is defined as follows:

$$L_p = \min_t \{ t : \phi(t) \leq p\phi(0) \}. \tag{2}$$

where $\phi(t)$ is the flux at time t, $\frac{\phi(t)}{\phi(0)}$ is the normalized flux (also known as lumen maintenance), and $\phi(0)$ is the nominal flux at time zero. In principle, samples of L_p can be obtained from Eq. (2) by observing sufficiently long degradation trajectories for ϕ. However, large depreciation events are seldom observed in practice and parametric models are necessary to extrapolate and characterize the uncertainty in the LED lifetime.

2.4. Thermoelectric degradation

Similarly to the TM-21 standard, [6], a modified exponential decay model is adopted in this work as follows:

$$\phi(t) = ae^{-(\alpha \times t)^{\beta}} \tag{3}$$

where a is the pre-exponential factor, α is the decay rate, and β is a shape parameter which modifies the TM-21 [6] model to better fit non-exponential trajectories.

In this work, the Arrhenius inverse power law is selected model thermoelectric ageing effects [36,37] due to its wide adoption in the research community. The model is defined as follows [37]:

$$\alpha(T, I) = bI^c e^{-\frac{E_a}{K_b}\frac{1}{T}}, \tag{4}$$

where b is the intercept parameter, c is a power exponent for the current, E_a is the activation energy, and K_b is the Boltzmann constant. Note that other accelerated ageing models can be used to capture interaction effects between the flux degradation and other stressors, e.g., the Eyring model, the Black model, and the Hellberg–Peck hygro-thermal-electrical model and others [38–42]. Note that an appropriate model must be selected to optimize fitting performance, however, model selection is not the main focus of this work and thus not further discussed here.

Once the fitting parameters are estimated, the LED lifetime can be obtained as:

$$L_p(T, I) = \frac{\left(\ln(\frac{a}{p})\right)^{\frac{1}{\beta}}}{\alpha(T, I)}, \tag{5}$$

where L_p is the long-term (extrapolated) luminous flux maintenance life for a maximum depreciation level p.

2.5. Linearized inverse power law model

By taking the logarithm of Eq. (4), an expression for log-decay rate is obtained as follows:

$$\ln(\alpha) = \ln(b) + c\ln(I) - \frac{E_a}{K_b}\frac{1}{T}, \tag{6}$$

where $\ln(\alpha)$ decreases linearly with $\frac{1}{T}$ and increases linearly with $\ln(I)$. Similarly, taking twice the logarithm of Eq. (3) and applying Eq. (6), the following linearized inverse power model is obtained [36]:

$$\ln\left(\ln\left(\phi\right)\right) = \theta_1 + \theta_2\ln(I) + \frac{\theta_3}{T} + \theta_4\ln(t), \tag{7}$$

where θ is the re-parameterized set of fitting coefficients. Note that this model cannot capture interaction effects between T and I on the degradation, i.e., the linearized model is additive for T and I.

2.6. Baseline lifetime predictors

Several approaches have been proposed to characterize the flux data in $\mathcal{D}$ and predict L_p. In this work, the proposed IPM is tested against two well-established approaches, (i) a TM-21-11 model and (ii) a random coefficient model (RCM).

2.6.1. The TM-21 model

The TM-21-11 and the LM-84-14 standards [6,7] provide recommendations to model the degradation data in $\mathcal{D}$, where an ordinary least squares (OLS) of an exponential decay model combined with the thermal-electrical acceleration model is proposed. Then, UQ is achieved by a statistical analysis of the residuals and by applying an empirical correction (to account for small sample sizes).

In this work, similarly to the TM-21, a baseline approach is considered in this by work applying Eq. (7) and fits its parameter as follows:

$$y_{a,k,\tau} = \theta_a\psi^T(\mathbf{x}_{a,k,\tau}) + \epsilon_{a,k,\tau}, \quad \forall a \in [n_a], \tag{8}$$

where $\epsilon_{a,k,\tau}$ are the residuals for the accelerated stress conditions $a = 1,\dots,n_a$, the devices $k = 1,\dots,n_s$, and for the time indices $\tau = 1,\dots,n_t$, $\psi(\mathbf{x})$ is a non-linear transformation of explanatory variables, $y = \ln\left(\ln\left(\phi\right)\right)$ is the dependent variable, that is, twice the logarithmic of the flux data, and $\theta_a = (\theta_1, \theta_2, \theta_3, \theta_4)_a$ is the vector of regression coefficients for the accelerated condition a. The basis function $\psi(\mathbf{x}) = \left(1, \ln(I), \frac{1}{T}, \ln(t)\right)$ $\mathbf{x} = (t, T, I)$ transform the time, current, and temperature data and OLS identifies n_a optimized parameter vectors $\theta_a^\star$ by minimizing the sum of squared residuals $\sum_k\sum_\tau \epsilon^2_{a,k,\tau}$ for all $a = 1,\dots,n_a$. Unfortunately, this model can lead to inaccurate UQ if residuals are correlated, with non-zero mean, and non-constant variance. Furthermore, it does not provide a device-specific characterization of degradation trajectories.

2.6.2. The random coefficient model

A random coefficient model is a particular type of regression model with device-specific effects, see e.g. [43,44]. In this work, a RCM define by solving a linear panel regression problem for all $a = 1,\dots,n_a$ and $k = 1,\dots,n_s$ a as follows [43]:

$$y_{a,k,\tau} = \theta_{a,k}\psi^T(\mathbf{x}_{a,k,\tau}) + \epsilon_{a,k,\tau}, \quad \forall a \in [n_a], k \in [n_s], \tag{9}$$

where $\theta_{a,k}$ are regression parameters for the $k = 1,\dots,n_s$ LED components and for the $a = 1,\dots,n_a$ stressors combinations. The RCM parameters are obtained minimizing $\sum_\tau \epsilon^2_{a,k,\tau}$ for all $a = 1,\dots,n_a$ and $k = 1,\dots,n_s$. Then, realizations of L_p are extrapolated by applying Eq. (5). Then a Weibull distribution $F_{L_{p,a}}(t), a = 1,\dots,n_a$ are fit via maximum likelihood estimation and characterize the natural variability of lifetimes.

3. The proposed approach

Fig. 1 summarizes the proposed framework for quantifying aleatory and epistemic uncertainties and making interval-valued LED lifetime predictions. The process begins by collecting accelerated degradation data (flux) and selecting a degradation threshold p. The longitudinal samples in $\mathcal{D}$ are then transformed into interval-censored and right-censored L_p samples, as detailed in Section 4. If L_p data is available, typically when the lumen maintenance threshold p is sufficiently large, non-parametric models are used to characterize a set of distributions for L_p. These models are described in the subsequent section. On the other hand, if L_p data is unavailable, which is often the case for lumen maintenance thresholds $p < 0.9$ in real-life applications, the new IPM model is computed to generate interval-valued lifetime predictions. These predictions are then compared to the baseline models introduced in Section 2.6, and epistemic uncertainty is quantified using statistically guaranteed bounds on the IPM's error probability.

Note that IPMs equipped with a certificate of generalization error have been applied to several real-life problems like, robust uncertainty propagation [45], history matching [46], outliers removal [47], interval-prediction of frequency response functions [48], and to study crack growth with sparsely available fatigue data [49]. However, to the authors' best knowledge, IPMs for LED lifetime prediction and interval prediction of lumen maintenance have not been investigated yet.

3.1. Non-parametric lifetime model

Non-parametric Kaplan–Meier (KM) and Probability-box (P-box) survival models characterize the aleatory and epistemic uncertainty in the lifetimes when p is large and lifetime data available. For the mathematical definitions and additional details, the reader is reminded of the Appendix and [13,50–52]. Note that non-parametric models are useful if a sufficient number of failure events are collected, e.g., for high p the likelihood of observing L_p is higher hence allowing for a more robust UQ that does not require parametric model assumptions. On the other hand, lower thresholds p parametric models are required because of the almost complete unavailability of L_p samples.

3.2. Physics-informed IPM for LED lifetime predictions

Simple regression models may fail to characterize accurately the uncertainty affecting the long-term lumen maintenance and lifetime of LEDs. To overcome this limitation, an IPM is proposed to identify plausible ranges for the flux depreciation trajectories and lifetimes. The model assigns to a vector of explanatory variables $\mathbf{x}$ a range for the dependent variables as follows [48]:

$$\mathcal{I}(\mathbf{x};\theta) = [f(\mathbf{x};\theta_l), f(\mathbf{x};\theta_u)] = [f_l(\mathbf{x}), f_u(\mathbf{x})]. \tag{10}$$

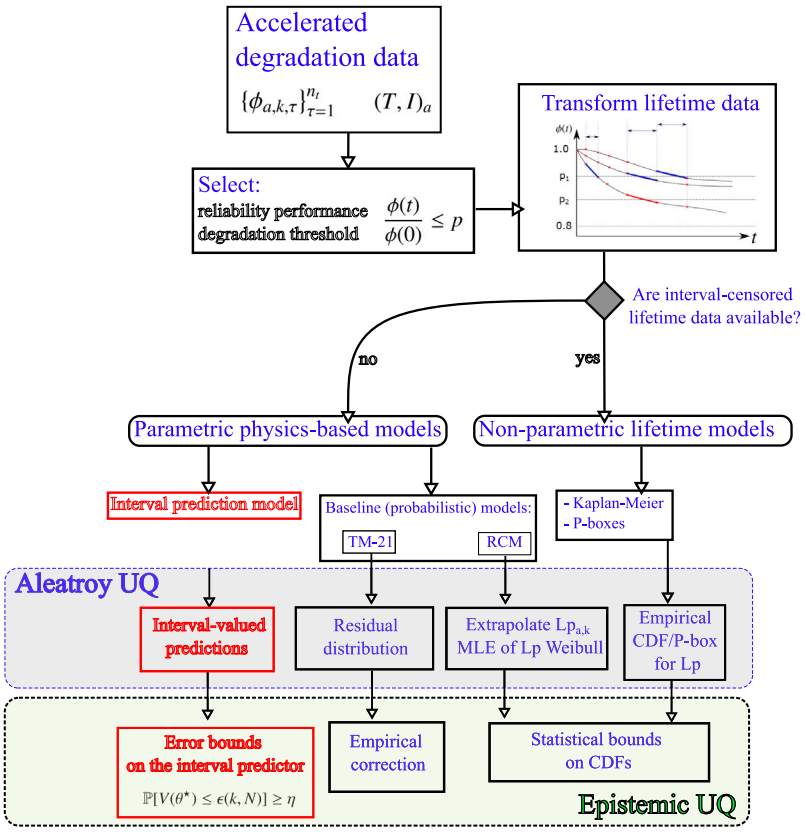

Fig. 1. A flowchart summarizing the structure of the proposed framework. The main novelty of this framework, i.e., the IPM model and epistemic UQ are highlighted in red color.

where the functions $f_l(\mathbf{x}) = f(\mathbf{x};\theta_l)$ and $f_u(\mathbf{x}) = f(\mathbf{x};\theta_u)$ characterization of the uncertainty in the output and are defined by a linear combination of fitting coefficients and basis as follows:

$$f(\mathbf{x};\theta) = \theta\psi^T(\mathbf{x}) = \sum_{k=1}^{n_\theta} \theta_k \psi_k(\mathbf{x}) \tag{11}$$

where a basis function, i.e. the non-linear transformation $\psi(x)$, embed within the model physical information of the degradation process. The known exponential decay and accelerated Arrhenius models. The IPM is uniquely identified by a vector of fitting coefficients $\theta = (\theta_l, \theta_u) \in \mathbb{R}^{n_\theta}$ and the variability in the flux depreciation trajectories is characterization via a set of possible depreciation paths. The parameter vector $\theta_l \in \mathbb{R}^{n_{\theta,l}}$ defined lower bounding function, $\theta_u \in \mathbb{R}^{n_{\theta,u}}$ are fitting coefficients for the function bounding the degradation process from above and the total number of IPM parameters is given by $n_\theta = n_{\theta,l} + n_{\theta,u}$.

3.2.1. Basis functions

The selection of appropriate basis functions ψ is a problem-dependent task. In principle, the function must be sufficiently complex to capture relevant dynamics in the degradation path and possibly embed within the IPM physical knowledge of the ageing process and natural variability in the data. In this work, basis functions are selected based on the linearized flux depreciation model and defined as follows:

$$\psi(\mathbf{x}_i) = \left(\psi_{1,i}, \psi_{2,i}, \psi_{3,i}, \psi_{4,i}\right) = \left(1, \ln(I_i), \frac{1}{T_i}, \ln(t_i)\right), \tag{12}$$

where $\mathbf{x}_i = (t_i, T_i, I_i)$ defines the ith sample for time, temperature, and current. Hence, this selection for the basis functions leads to a total number of IPM parameters $n_\theta = 8$, where $n_{\theta,l} = n_{\theta,u} = 4$.

3.2.2. Identification approach

The IPM is identified by constraining the samples in $\mathcal{D}$ to lay between the upper and lower bounds while optimizing a tightness condition on $\mathcal{I}(\mathbf{x};\theta)$, [53]. In this work, the vector θ is identified by solving the following optimization program:

$$\theta^\star = \arg\min_{\theta_u,\theta_l} \int_{\mathcal{X}} (\theta_u - \theta_l)\psi^T(\mathbf{x})\, dx$$

subject to

$$\begin{aligned} &\theta_l\psi^T(\mathbf{x}) \leq \theta_u\psi^T(\mathbf{x}) \;\forall\, \mathbf{x} \in \mathcal{X} \\ &y_i \geq \theta_l\psi^T(\mathbf{x}_i), \\ &y_i \leq \theta_u\psi^T(\mathbf{x}_i),\;\; i = 1,\ldots,N \end{aligned} \tag{13}$$

where $\theta^\star$ is the optimized parameters vector, N is the number of samples $(\mathbf{x}_i, y_i) \in \mathcal{D}$, and the objective function defines the area between the lower and the upper bound, proportional to the average width of the bounding interval $\mathcal{I}(\mathbf{x};\theta)$ to be minimized. Note that each sample in the data set defines two deterministic constraints in the optimization problem, one on the upper and one on the lower bounding function. The last constraint ensures the dominance of the upper bound in prediction region $\mathcal{X}$, which is necessary for long-term extrapolation of L_p for times beyond the test duration. Optimization program (13) is linear in the regression coefficients θ and a solution can be obtained very efficiently using standard linear programming solvers. For further details on the numerical implementation the interested reader is reminded to [48].

3.2.3. Statistical bounds on the error probability

The accuracy of the IPM is the probability of new samples falling within the computed bounds as given by:

$$P_a(\theta) = \mathbb{P}[(\tilde{\mathbf{x}}, \tilde{y}) : \tilde{y} \in \mathcal{I}(\tilde{\mathbf{x}};\theta)], \tag{14}$$

where $(\tilde{\mathbf{x}}, \tilde{y})$ is a new sample, i.e., a test condition $\tilde{\mathbf{x}}$ and twice the logarithm of the corresponding flux measurement $\tilde{y}$. The violation probability $V(\theta) = 1 - P_a(\theta)$ defines the error probability of the IPM

Table 1
A summary of the .csv data sheets with table sizes, test duration, number of samples, number of distinct LED technologies, and number of accelerated stressors. The data sets are available online at https://github.com/Roberock/Degradation-data-LED-packages-and-lamps.git.

Data ID	Type	n_{tech}	n_a	H $\times 10^3$	n_t	n_s	*Size*	Ref
1	IES-LM-80	25	$\in [2, 12]$	$\in [6, 18]$	$\in [7, 19]$	$\in [12, 30]$	$[43105 \times 9]$	[1,2]
2	IES-LM-80	1	5	10	$\in [12, 20]$	$\in [12, 30]$	$[2454 \times 12]$	[1,2]
3	Other	1	1	1.6	72	16	$[1152 \times 5]$	[55,56]
4	Other	1	1	2.16	10	5	$[50 \times 411]$	[57]
5	IES-LM-80	1	6	$\in [6, 14]$	$\in [13, 29]$	$\in [19, 25]$	$[3006 \times 6]$	[58]
6	IES-LM-80	1	3	$\in [6, 10]$	$\in [7, 11]$	25	$[725 \times 8]$	[58]

and a sample-based estimator is given by

$$\hat{V}(\theta) = \frac{\sum_{i=1}^{n} \mathbf{1}\{\tilde{y}_i \notin \mathcal{I}(\tilde{\mathbf{x}}_i; \theta)\}}{n},$$

where $\mathbf{1}\{c_i\}$ is the indicator function for the event $\{c_i\}$ and n is the number of samples used for the estimation. In practice, the true $V(\theta)$ is always unavailable and a lack of validation samples further complicates the analysis. In this work, a non-asymptotic and distribution-free generalization error bound is defined as follows [54]:

$$\mathbb{P}[V(\theta^\star) \leq \epsilon(k, N)] \geq \eta,$$

where $\theta^\star$ is optimized in Eq. (13), η is a confidence level, and N denotes the number of samples used in the optimization. The bound $\epsilon(k, N)$ is an upper bound on the reliability $V(\theta^\star)$, i.e., a quantifier of the epistemic uncertainty associated with the error probability. The quantity k represents the minimum number of data points required to reproduce the optimum and relates to the complexity of $\theta^\star$ and for convex programs such as (13), $k \leq n_\theta$ where n_θ is the number of regression parameters. Therefore, $\epsilon(n_\theta, N)$ provides a conservative bound on the error probability of $\mathcal{I}(\mathbf{x}; \theta^\star)$ and gets tighter, i.e., reduces the epistemic uncertainty associated with the lifetime predictions, for larger N and simpler models, i.e., for lower n_θ and k. These bounds assume stationary $\mathbb{P}$ and a consistency optimizer, e.g., see [54]. Nevertheless, specific assumptions on the distribution family of the data are not required. It is important to note that the bound is specifically defined for $\theta^\star$ optimized from a random realization of a data set $\mathcal{D}$, making it a data-dependent bound.

4. A novel database for LED reliability analyses

A new database has been compiled for the analysis of LED lifetime, consisting of six sets of constant-stress accelerated degradation trajectories for high- and medium-power LED packages and lamps. The database contains over 50 thousand measurements, covering 29 distinct LED technologies obtained from accelerated reliability qualification experiments, including LM-80 and other tests. The dataset includes both high-power packages, operating at a normal current of 250–300 mA, and mid-power LEDs with normal current ranging from 50 to 250 micro Amperes. Its primary purpose is to serve as a testing and validation platform for new LED reliability and durability assessment methods.

Table 1 provides a summary of the available data, including different ageing and degradation indicators, test duration, sample sizes, LED types, and thermoelectrical stress levels. The table lists the identifier for each dataset, the number of LED technologies available (n_{tech}) and the range of LED technologies covered (n_a), the duration of the experiments expressed in thousands of hours (H), the number of samples for each degradation trajectory (n_t), and the number of tested devices for each stress condition (n_{sam}). A size in tabular form for each dataset and references are also supplied.

Similarly, in Table 2, available reliability performance indicators are presented, including correlated color temperature (CCT) and spectral power density (SPD). The table also indicates whether raw (non-normalized) flux data is available as well as the availability of other features, e.g., $CCT(0)$ at time 0 and whether one, both or none of the stressors T and I are available.

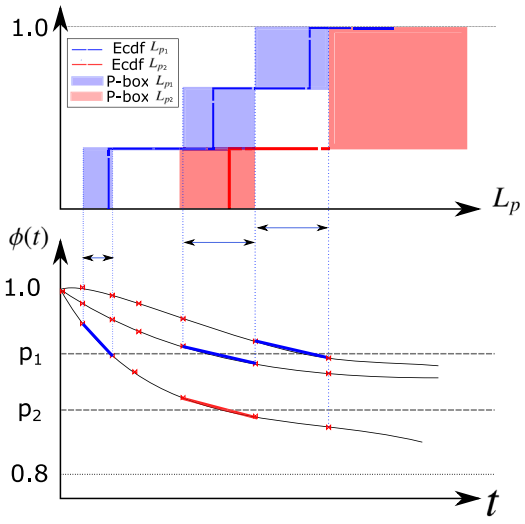

Fig. 2. A graphical example illustrating the conversion of three flux degradation trajectories into L_p data and non-parametric P-boxes. The resulting p-boxes and empirical distributions for the threshold levels p_1 and p_2 are represented by blue and red lines, respectively.

A numerical procedure is designed to extract L_p data from longitudinal lumen maintenance samples, i.e., from the normalized flux measurements $\frac{\phi(t)}{\phi(0)}$. The procedure yields two data sets: (i) a collection of point-valued L_p samples and right-censoring indicators and, (ii) a set of interval-censored and right-censored data for L_p. Data set (ii) is computed by first selecting a depreciation threshold p and identifying time windows corresponding to the first passage time. If the window exists, L_p is interval-censored within this time interval, otherwise, the sample of L_p equals the test duration and a right-censoring indicator is assigned.

Data set (i) is computed similarly to (ii) but assumes linear flux between consecutive flux measurements and thus replaces the interval data with a point-valued L_p. Note that (ii) is obtained directly from the data without any assumption on the degradation paths between consecutive measurements. The procedure is conceptually depicted in Fig. 2 where the data from three degradation paths are converted into a data set (i) and (ii) and then the empirical distributions and P-boxes for L_p are computed. Specifically, two flux depreciation thresholds p_1 and p_2 are selected and the corresponding distributions are displayed in blue and red, respectively. Refer to the Appendix for two examples of L_p data (i) and (ii) extracted as previously described.

5. Analyses, results, and discussions

The uncertainty of both low-magnitude and high-magnitude flux depreciation events is quantified using parametric and non-parametric reliability models on the test data set (Section 4). The following analyses are conducted on a local machine equipped with an Intel(R) Core(TM) 1.80 GHz processor and 32 GB RAM, using MATLAB (R2022b) and a modified version of the software package [48], which incorporated the *linprog* function for IPM identification.

Table 2
A summary of the measured response variables, accelerating factors and other device-specific parameters. Availability of raw data (✓), or if only normalized flux is available is also reported.

Data ID	LED type	Degradation indicator	Stressors	Other features	Raw data
1	MP/HP package	$\phi(t)$	T, IF	Material, Die, $CCT(0)$	–
2	MP package	$\phi(t)$, $\Delta u'v(t)$	T, IF	$CCT_{x,y}(0)$, $\phi(0)$, $V_f(0)$	✓
3	HP package	$\phi(t)$, $\Delta u'v(t)$	–	–	–
4	Lamp	$\phi(t)$, $\Delta u'v(t)$, $SPD(t)$, $CCT(t)$	T	–	✓
5	HP package	$\phi(t)$	T, IF	–	–
6	HP package	$\phi(t)$	T	$\phi(0)$, $V_f(0)$	✓

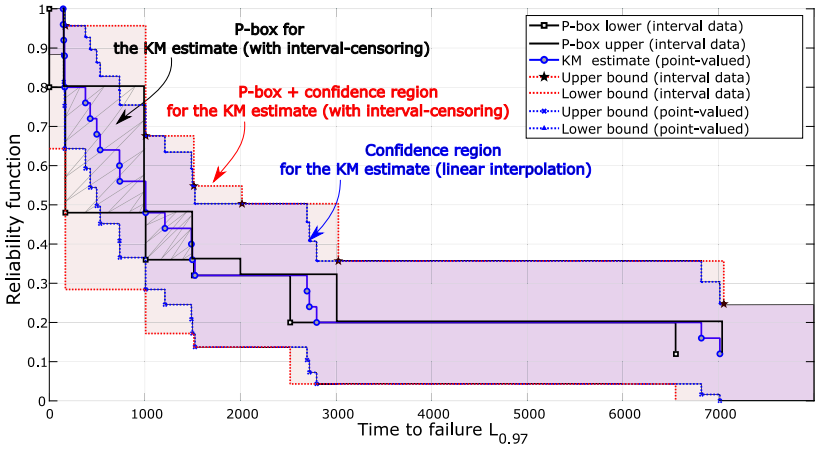

Fig. 3. The KM estimate and confidence bounds on the reliability function for $L_{0.97}$ and for $T = 105$ Celsius and $I = 350$ $[mA]$. The linear interpolation data in Table 5 is presented by blue curves whilst the probability box derived from interval-censored data (and confidence bounds) are displayed by black and red lines, respectively.

5.1. Non-parametric KM and P-box models

The uncertainties in low-magnitude degradation events are quantified using a lumen maintenance threshold of $p = 0.97$, i.e., a maximum 3% lumens depreciation. Data for $L_{0.97}$ is obtained from data set ID 1 under stress conditions of 105 Celsius and 350 mA. The KM and P-box estimators, computed without relying on parametric model assumptions, are obtained from the censored data in Table 5 and Table 6, respectively. Fig. 3 shows the resulting KM (solid and dashed blue line) and P-box (solid black lines) reliability estimators with their 95% confidence regions, respectively, in blue and red. Note that the black P-box accounts for measurement imprecision caused by interval censoring, while the confidence region in red considers also epistemic uncertainty from lack of samples. Analyzing the confidence regions, we find that at hour 500, the KM estimator bounds the probability of lumen retained flux higher than 97% between 0.45 and 0.828. In contrast, the P-box indicates a probability range of 0.28 to 0.956. The KM estimate's confidence interval lies within the P-box and is tighter, indicating lower uncertainty. This discrepancy arises from the assumptions made on flux degradation paths, such as linear interpolation between measurements, necessary for computing point-valued L_p realizations and the KM estimate. This result highlights how unwarranted assumptions can lead to underestimated uncertainty and potentially incorrect conclusions regarding L_p. Similar analyses are conducted for other p levels (0.98, 0.97, and 0.96) and data sets. However, the epistemic uncertainty (width of confidence region) bounds remain unaffected. Longer test durations can decrease right-censoring rates and enhance the non-parametric characterization of L_p, however, to reduce the epistemic uncertainty, larger sample sizes and more frequent measurements within shorter measurement windows(lower interval-censoring) may be required. Practical and industrial constraints, such as budget and time limitations, often make this challenging to achieve.

5.2. Results for the TM-21 and RCM

The baseline models in Section 2.6 are applied to the data ID 1 to predict the L_p of LED type 1 for three different thresholds $p = 0.7, 0.8, 0.9$. The data consist of $n_a = 9$ combinations of temperature and current, along with 25 degradation paths for each condition. Following the TM-21/28 recommendations, burn-in data is discarded, and only measurements taken after 5000 h are considered if at least 10000 h of test data are available. The TM-21 approach, represented by Eq. (8), produces nine models, one for each stressor combination, whilst the RCM in Eq. (9), yields 225 models. The TM-21 model extrapolates L_p and lower confidence bounds at a 95% confidence level attained by assuming normally distributed residuals. The RBC model yeld 25×9 lifetimes extrapolations a Weibull distribution $F_{L_{p,a}}$ computed for all $a = 1, \ldots, 9$ and $p = 0.7, 0.8, 0.9$. Fig. 4 presents the Weibull's probability plot for 4 accelerated conditions (sub-panels) and the markers indicate the extrapolated L_p values. Although Weibull distributions generally fit the data well for high values of the stressors, they provide a poorer fit at lower stress levels and particularly on the tails of the distribution.

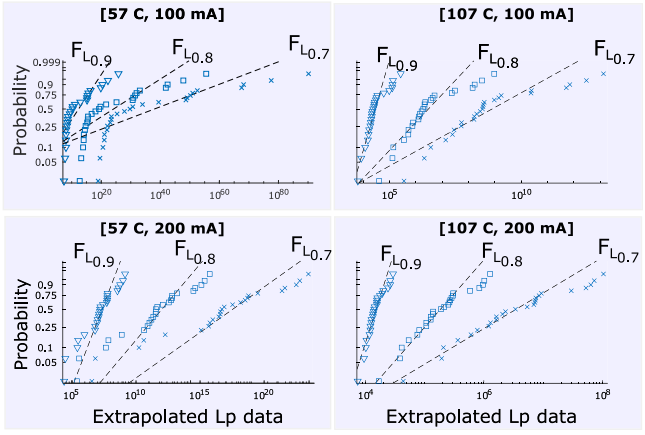

Fig. 4. Probability plots for the Weibull lifetime distributions $F_{L_{0.9}}$, $F_{L_{0.8}}$, and $F_{L_{0.7}}$. The four selected (T, I) combinations are displayed in the four panels.

Table 3
A comparison between the lower bounds on the L_p predictions of the TM-21 model, RCM and the proposed IPM for $p = 0.9,\ 0.8$, and 0.7. Each row corresponds to one of the nine available accelerated stress levels.

		TM-21			RCM + Weibull			IPM		
		$L_{0.9}$	$L_{0.8}$	$L_{0.7}$	$L_{0.9}$	$L_{0.8}$	$L_{0.7}$	$L_{0.9}$	$L_{0.8}$	$L_{0.7}$
T [°C]	I [mA]	[h] $\times 10^5$								
57	100	>10	>10	>10	>10	>10	>10	>10	>10	>10
88	100	6.36	>10	>10	4.40	9.40	>10	0.25	5.88	>10
107	100	0.17	3.22	>10	0.03	3.37	8.95	0.07	0.41	3.64
57	150	>10	>10	>10	>10	>10	>10	>10	>10	>10
88	150	1.55	>10	>10	2.61	8.40	>10	0.19	2.54	>10
107	150	0.31	>10	>10	0.056	>10	>10	0.17	>10	>10
57	200	4.09	>10	>10	3.76	9.08	>10	0.28	3.95	>10
88	200	0.22	1.64	>10	0.068	1.68	9.50	0.13	0.71	5.68
107	200	0.11	0.62	4.24	0.066	0.35	5.50	0.05	0.155	0.47

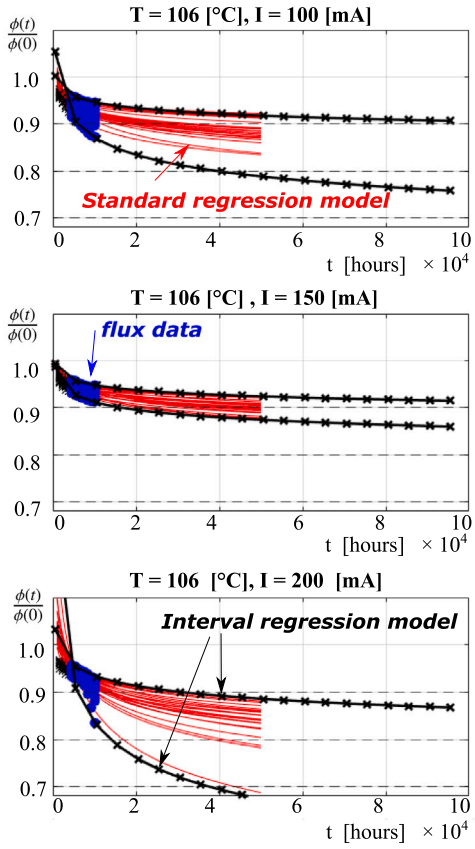

Fig. 5. The IPM lumen depreciation bounds, the black marked lines, and the results of the random coefficient model, the solid red lines, for three accelerated conditions in the sub-panels. The blue markers display the normalized flux data (set ID 1) used to fit both models.

It is worth noting that while the shape of the data distribution may be similar for different p values, the variance of the distribution noticeably increases for higher $1 - p$ and (I, T) combinations. This indicates non-constant flux variance across time and in the space of accelerating factors.

5.2.1. Interval-valued L_p predictions

The IPM is applied to the flux decay data, and the samples with $t > 5000$ hours define the constraints in program (13). The identification method produces two bounding functions on the flux decay trajectories, and the optimal $\theta^\star$ defines the bounds. As intended, the IPM fully envelops the data, with $f_u \geq f_l$ in the prediction region. Fig. 5 presents the optimized IPM $\mathcal{I}(x; \theta^\star)$ (black marked lines) for three acceleration levels, while the blue markers display the available flux data. The red curves show the results of the random coefficient model used in the previous section to extrapolate service life and characterize the L_p distributions. It is noteworthy that the regression band is generally wider for high T and I, indicating higher variability and non-constant variance in the space of accelerating factors. The last nine rows of shows the lower L_p prediction obtained inverting $f_l(x; \theta^\star)$ for $p = 0.9$, 0.8, and 0.7, along with the nine stress levels. Similar to the results of traditional probabilistic approaches, low acceleration rates lead to $L_p > 10^6$, suggesting higher durability of this LED. On the other hand, high temperatures substantially accelerate the flux decay process, resulting in a shorter lumen maintenance life. For instance, the stress level $(T, I) = (107, 0.20)$ has a $L_{0.7}$ bound of 4.7×10^4 h.

5.2.2. Epistemic UQ and error bounds

The robustness and epistemic uncertainty in the interval model, $\mathcal{I}(\mathbf{x}; \theta^\star)$, are evaluated by assessing the error bound in Section 3.2.3. The IPM has $n_\theta = 8$ regression parameters (see Eqs. (7)) and because program (13) is linear (convex) the a-posteriori complexity of the model bounded by $k \leq 8$. The combination of model complexity and the number of training samples allows for obtaining an upper bound on the error probability. Table 4 displays the bounds $\epsilon(k, N)$ computed for a confidence level of $\eta = 0.999$, with different sample sizes, N, and model complexities, k. The chosen confidence level is very high, indicating a nearly certain probabilistic robustness guarantee. Due to the model having eight support scenarios, the error probability $V(\theta^\star) \leq 0.9418$ if $N = 10$ samples are used to identify the IPM and it lower to $V(\theta^\star) \leq 0.443$ for $N = 25$. The former bound approaches a non-informative interval due to the small sample size compared to the model complexity, resulting in high epistemic uncertainty. On the other hand, the model guarantees improve significantly for larger sample sizes and simpler models (lower k). For example, the violation probability bound tightens to $V(\theta^\star) \leq 0.0520$ for $N = 225$ and $k = 8$. Furthermore, if a simpler model with $k = 2$ is chosen, the violation probability bound improves even further to a value of 0.0150. In other words, a simple interval model with $k = 2$ (i.e., a linear model) trained with $N = 225$ degradation paths can guarantee that at least 98.5% of future flux degradation paths will fall within the predictive strip. Conversely, if the model is more complex ($k = 8$) and trained with fewer samples ($N = 25$), the accuracy bound deteriorates to 55.70%. As expected, lower epistemic uncertainty can be achieved with higher sample sizes. However, the complexity of the model also plays a role, as more complex models are generally less guaranteed due to their increased susceptibility to overfitting the data.

6. Conclusions and future research

This study introduced a novel framework for uncertainty quantification and lifetime predictions of light-emitting diodes (LEDs). Parametric and non-parametric models were used to characterize both aleatory

Table 4
Probabiltiy bounds $\epsilon(k, N)$ computed using the Wait-and-Judge method [54], assuming a very high confidence $\eta = 0.999$ and for different samples sizes, N, and different a-posteriori (data-dependent) complexity, k.

Reliability bound $\epsilon(k, N)$ for a confidence level $\eta = 0.999$								
Complexity	Sample size							
	$N = 10$	$N = 25$	$N = 50$	$N = 75$	$N = 100$	$N = 150$	$N = 200$	$N = 225$
$k = 2$	0.3215	0.1328	0.0671	0.0449	0.0337	0.0225	0.0169	0.0150
$k = 3$	0.4532	0.1901	0.0964	0.0646	0.0485	0.0324	0.0243	0.0216
$k = 4$	0.5733	0.2444	0.1244	0.0834	0.0627	0.0419	0.0315	0.0280
$k = 5$	0.6831	0.2965	0.1515	0.1017	0.0765	0.0512	0.0385	0.0342
$k = 6$	0.7824	0.3469	0.1779	0.1195	0.0900	0.0602	0.0453	0.0402
$k = 7$	0.8698	0.3956	0.2037	0.1370	0.1032	0.0691	0.0519	0.0462
$k = 8$	0.9418	0.4430	0.2290	0.1542	0.1162	0.0778	0.0585	0.0520

and epistemic uncertainty associated with various lumen depreciation levels. The framework was validated using real-world data from LM-80 accelerated stress tests. The results confirmed that the variance of the degradation trajectories is non-constant, both in terms of acceleration factors and over time, and that lumen maintenance predictions can still exhibit high levels of uncertainty, even for low-magnitude depreciation events. A linear model was established to link accelerated temperature and scale parameters of Weibull lifetime distributions, showing consistent results across twenty-five LED technologies. A comparison between the proposed interval prediction model and a well-established model indicated a comparable accuracy, with enhanced uncertainty quantification capabilities. Also, note that the IPM can capture the overall degradation trend in a group of LEDs but it cannot predict future trends in the degradation of specific devices, i.e., it does not account for variations and individual characteristics of specific devices.

Hybrid PHM frameworks that combine AI with advanced uncertainty quantification capabilities hold great promises for the future of the lighting industry. However, the effective deployment of AI models for LED prognostics faces many challenges, e.g., limited availability of degradation data, unlabeled failures, and a lack of dedicated pipelines for data storage, cleaning, and processing. Future research should focus on better exploiting historical and monitoring data, and on integrating complex physics-based models into physics-informed AI pipelines. There is a need to explore new models that can assess interaction effects between multiple stressors, quantify aleatory and epistemic uncertainties while predicting future LED-specific degradation paths. These innovative digital twin solutions, possibly embedding new degradation indicators, feature extraction tools, and efficient data collection strategies, are necessary to advance the state-of-the-art concerning LED lifetime prediction and uncertainty quantification.

CRediT authorship contribution statement

Roberto Rocchetta: Writing – original draft, Visualization, Validation, Software, Methodology, Data curation, Conceptualization. **Zhouzhao Zhan:** Writing – review & editing. **Willem Dirk van Driel:** Writing – review & editing, Resources, Funding acquisition. **Alessandro Di Bucchianico:** Supervision, Resources, Project administration, Funding acquisition.

Declaration of competing interest

The authors declare that they have no known competing financial interests or personal relationships that could have appeared to influence the work reported in this paper.

Data availability

Please refer to the github repository (see the link to the webpage in the manuscript).

Acknowledgments

We wish to acknowledge the gracious support of this research through the project '*AI powered Digital twin for lighting infrastructure in the context of front-end Industry 4.0*', AI-TWLIGHT, that has received funds from the ECSEL Joint Undertaking (JU) under grant agreement No 101007319. The JU receives support from the European Union's Horizon 2020 research and innovation program between the Netherlands, Hungary, France, Poland, Austria, Germany, Italy, and Switzerland. Note that this work reflects only the author's view and that the JU is not responsible for any use that may be made of the information it contains.

Appendix. Parametric and non-parametric reliability models

Methods that do not assume a specific reliability distribution family are known as non-parametric (or distribution-free) methods whilst a parametric method assumes a family for a lifetime distribution, $F(t;\theta)$. The reliability function is defined as $R(t;\theta) = 1 - F(t;\theta)$.

Likelihood estimation from censored data

By assuming iid lifetimes of the n items, the likelihood for type-II right-censored observations is defined as follows:

$$L(t_1, \dots, t_n; \theta) = \frac{n!}{(n-k)!} \left(\prod_{i=1}^{k} f(t_i;\theta) \right) R(t_k;\theta)^{n-k}. \tag{15}$$

Note that for type-I censoring, the number of failed items k is random while the experiment duration is fixed and equal to H. For interval-censored observations, $t_i \in [a_i, b_i]$, a likelihood function that combines interval-censored and right-censored data is given by:

$$L(t_1, \dots, t_n; \theta) \propto \left(\prod_{i=1}^{n} f(t_i;\theta)^{\delta_{1,i}} \right) \times \left(\prod_{i=1}^{n} (F(b_i;\theta) - F(a_i;\theta))^{\delta_{2,i}} \right) \left(\prod_{i=1}^{n} R(H;\theta)^{\delta_{3,i}} \right), \tag{16}$$

where $\delta_1, \delta_2, \delta_3$ are (censoring) indicators for point-valued x_i, interval-censored, $t_i \in [a_i, b_i]$, or type I right-censored data $t_i > H$, respectively.

Non-parametric Kaplan–Meier estimator

The non-parametric Kaplan–Meier estimator is used to characterize the reliability function from lifetime data with independent random censoring, i.e., from n pairs $\{t'_i, \delta_i\}_{i=1}^{n}$ where δ are right-censoring indicators and t' are time-to-failure data. The KM estimator is given by [50]:

$$\hat{S}(t) = \prod_{j:t_j \le t} \frac{r_j - d_j}{r_j} = \prod_{j:t_j \le t} \left(1 - \frac{d_j}{r_j}\right), \tag{17}$$

where $\delta_i = 1$ indicate a failure occurrence and $\delta_i = 0$ a censored observation, $t_1 < t_2 < \cdots < t_k$ are unique ordered values of $t'_1, \dots, t'_n$ and $d_j = \sum_{i=1}^{n} \delta_i \mathbf{1}\{t'_i = t_j\}$ and $r_j = \sum_{i=1}^{n} \mathbf{1}\{t'_i \ge t_j\}$.

Table 5
This table presents the time-to-first-first passage and right-censoring indicators for a $p = 0.97$ depreciation threshold, the data set with ID 5, and by assuming linear interpolation between consecutive measurements.

	$p = 0.97$											
T [°C]	55	85	85	105	85	105	55	85	85	105	85	105
I [A]	0.5	0.5	0.75	0.35	0.25	0.25	0.5	0.5	0.75	0.35	0.25	0.25
ID	Time-to-event L_p [h] (from the interpolation)						Right-censoring indicator					
1	3444.0	4516.2	3356.1	1486.4	3956.4	1225.3	0	0	0	0	0	0
2	9942.5	6757.9	3415.2	1209.6	2196.0	1959.3	0	0	0	0	0	0
3	3143.4	4314.7	1768.3	11 000.0	13 500.0	14 000.0	0	0	0	1	1	1
4	2989.0	6552.0	1024.8	144.8	4506.7	1450.3	0	0	0	0	0	0
5	2948.9	4302.4	1556.0	161.5	7807.9	1197.0	0	0	0	0	0	0
6	6012.0	4852.0	1670.1	1496.6	1985.3	2308.9	0	0	0	0	0	0
7	4032.0	10 399.7	344.8	1523.7	8852.2	9558.0	0	0	0	0	0	0
8	2833.6	10 251.1	1663.2	159.5	8946.0	1449.0	0	0	0	0	0	0
9	10 080.0	9937.4	555.7	11 000.0	4413.7	2160.0	1	0	0	1	0	0
10	5555.0	3745.1	6048.0	161.5	13 500.0	14 000.0	0	0	1	0	1	1
11	3449.6	11 000.0	6048.0	2720.3	5242.8	147.4	0	1	1	0	0	0
12	9001.6	4748.0	3897.6	11 000.0	4506.4	2450.5	0	0	0	1	0	0
13	3976.6	988.5	4421.2	6821.3	13 500.0	13 407.9	0	0	0	0	1	0
14	6517.2	4923.2	1504.9	150.9	2384.6	7692.6	0	0	0	0	0	0
15	3764.4	3598.3	4439.1	1008.0	8531.3	2772.0	0	0	0	0	0	0
16	8991.5	2499.6	6048.0	737.7	1825.1	2386.5	0	0	1	0	0	0
17	5796.0	8327.0	4278.4	496.1	13 500.0	12 940.5	0	0	0	0	1	0
18	3658.1	916.9	6048.0	2796.7	13 500.0	14 000.0	0	0	1	0	1	1
19	10 080.0	7803.5	6048.0	2695.8	1808.7	1864.5	1	0	1	0	0	0
20	4880.8	4004.0	6048.0	1008.0	13 500.0		0	0	1	0	1	
21		2114.0	6048.0	378.0				0	1	0		
22		3612.0	164.7	532.2				0	0	0		
23		2797.2	6048.0	7015.1				0	1	0		
24		1309.2	6048.0	734.3				0	1	0		
25		9112.6	6048.0	427.6				0	1	0		

Table 6
A table of interval- and right-censored flux depreciation events for a failure threshold of $p = 0.97$, data set ID 5, and without any assumption on the flux depreciation trajectories in-between measurements.

	$p = 0.97$											
T [°C]	55		85		85		105		85		105	
I [A]	0.5		0.5		0.75		0.35		0.25		0.25	
ID	Time-to-event L_p [h] (interval-censored and right-censored)											
1	3024	3528	4032	4536	3024	3528	1008	1512	3528	4032	1008	1512
2	9576	10080	6552	7056	3024	3528	1008	1512	2016	2520	1512	2016
3	3024	3528	4032	4536	1512	2016	11000	Inf	13500	Inf	14000	Inf
4	2520	3024	6048	6552	1008	1512	0	168	4032	4536	1008	1512
5	2520	3024	4032	4536	1512	2016	0	168	7560	8064	1008	1512
6	5544	6048	4536	5040	1512	2016	1008	1512	1512	2016	2016	2520
7	3528	4032	10080	10500	168	1008	1512	2016	8568	9072	9072	9576
8	2520	3024	10080	10500	1512	2016	0	168	8568	9072	1008	1512
9	10080	Inf	9576	10080	168	1008	11000	Inf	4032	4536	2016	2520
10	5544	6048	3528	4032	6048	Inf	0	168	13500	Inf	14000	Inf
11	3024	3528	11000	Inf	6048	Inf	2520	3024	5040	5544	0	168
12	8568	9072	4536	5040	3528	4032	11000	Inf	4032	4536	2016	2520
13	3528	4032	168	1008	4032	4536	6552	7056	13500	Inf	13000	13500
14	6048	6552	4536	5040	1008	1512	0	168	2016	2520	7560	8064
15	3528	4032	3528	4032	4032	4536	168	1008	8064	8568	2520	3024
16	8568	9072	2016	2520	6048	Inf	168	1008	1512	2016	2016	2520
17	5544	6048	8064	8568	4032	4536	168	1008	13500	Inf	12500	13000
18	3528	4032	168	1008	6048	Inf	2520	3024	13500	Inf	14000	Inf
19	10080	Inf	7560	8064	6048	Inf	2520	3024	1512	2016	1512	2016
20	4536	5040	3528	4032	6048	Inf	168	1008	13500	Inf		
21			2016	2520	6048	Inf	168	1008				
22			3528	4032	0	168	168	1008				
23			2520	3024	6048	Inf	6552	7056				
24			1008	1512	6048	Inf	168	1008				
25			9072	9576	6048	Inf	168	1008				

Non-parametric empirical P-boxes

A P-box defines a lower and upper CDF $[\underline{F}(x), \overline{F}(x)]$ and can be parametric or non-parametric, depending on whether the family for $F(x)$ is specified or not. A non-parametric P-boxes is built from interval-censored lifetime data as follows:

$$\hat{\underline{F}}(t) = \frac{1}{n}\sum_{i=1}^{n} \mathbf{1}_{b_i \leq t} \ , \quad \hat{\overline{F}}(t) = \frac{1}{n}\sum_{i=1}^{n} \mathbf{1}_{a_i \leq t} \ , \tag{18}$$

where a_i and b_i are lower and upper bounds of interval-censored data. For a mixture of interval- and right-censored data, two KM estimation on the sets of lower and upper bounds allows obtaining a P-box for the reliability function, i.e., $[\hat{\underline{S}}(t), \hat{\overline{S}}(t)]$. The interested reader is reminded to [51] for more details on methods to construct P-boxes from censored data.

Censored L_p data

Table 5 shows an example of survival data (i) extracted as described in Section 4 from the dataset ID 5 and by selecting a very high threshold $p = 0.97$. The columns show the outcomes for the six accelerated stress levels. Table 6 shows an example of survival data (ii) for the same data but without any assumption on the degradation trajectories. For each sample, only intervals on the L_p are available and *inf* values indicate a right-censored failure event.

References

[1] Fan X, Van Driel W. Solid state lighting reliability: components to systems. Springer; 2013.

[2] Van Driel WD, Fan X, Zhang GQ. Solid state lighting reliability Part 2. Springer; 2017.

[3] Chang M-H, Das D, Varde P, Pecht M. Light emitting diodes reliability review. Microelectron Reliab 2012;52(5):762–82. http://dx.doi.org/10.1016/j.microrel.2011.07.063.

[4] Nogueira E, Vazquez M, Mateos J. Accelerated life test of high luminosity AlGaInP LEDs. Microelectron Reliab 2012;52(9):1853–8. http://dx.doi.org/10.1016/j.microrel.2012.06.125, Special Issue: 23rd European symposium on the reliability of electronic devices, failure physics, and analysis.

[5] Meneghini M, Dal Lago M, Trivellin N, Mura G, Vanzi M, Meneghesso G, Zanoni E. Chip and package-related degradation of high power white LEDs. Microelectron Reliab 2012;52(5):804–12. http://dx.doi.org/10.1016/j.microrel.2011.07.091.

[6] America I. Projecting long term lumen maintenance of LED light sources. New York (NY): Illuminating Engineering Society; 2011.

[7] Committee ITP, et al. IES TM-28-14: Projecting long-term luminous flux maintenance of LED lamps and luminaire. New York, NY, USA: Illuminating Eng. Society; 2014.

[8] Kuebler B, Jackson A, Randolph DN, Jiao J, et al. ANSI/IES TM-35-19: Projecting long-term chromaticity coordinate shift of LED packages, arrays and modules. Illuminating Engineering Society; 2019.

[9] Commission IE, et al. IEC/PAS 62717 LED modules for general lighting–performance requirements. IEC SDAR J 2015.

[10] Bui DA, Hauser PC. Analytical devices based on light-emitting diodes – a review of the state-of-the-art. Anal Chim Acta 2015;853:46–58.

[11] Gray A, Wimbush A, de Angelis M, Hristov PO, Calleja D, Miralles-Dolz E, Rocchetta R. From inference to design: A comprehensive framework for uncertainty quantification in engineering with limited information. Mech Syst Signal Process 2022;165:108210.

[12] Magnien J, Dvorzak M, Kleb U, Mücke M, Kraker E. Probabilistic approach for temperature driven fatigue lifetime data analysis to improve prognostics and health management of LED packages. In: 2020 26th International workshop on thermal investigations of ICs and systems (THERMINIC). IEEE; 2020, p. 173–9.

[13] Rocchetta R, Broggi M, Patelli E. Do we have enough data? Robust reliability via uncertainty quantification. Appl Math Model 2018;54:710–21. http://dx.doi.org/10.1016/j.apm.2017.10.020.

[14] Kim DW, Oh H, Youn BD, Kwon D. Bivariate lifetime model for organic light-emitting diodes. IEEE Trans Ind Electron 2017;64(3):2325–34. http://dx.doi.org/10.1109/TIE.2016.2623584.

[15] Qu X, Wang H, Zhan X, Blaabjerg F, Chung HS-H. A lifetime prediction method for LEDs considering real mission profiles. IEEE Trans Power Electron 2017;32(11):8718–27. http://dx.doi.org/10.1109/TPEL.2016.2641010.

[16] Fan J, Jing Z, Cao Y, Ibrahim MS, Li M, Fan X, Zhang G. Prognostics of radiation power degradation lifetime for ultraviolet light-emitting diodes using stochastic data-driven models. Energy and AI 2021;4:100066. http://dx.doi.org/10.1016/j.egyai.2021.100066.

[17] Fan J, Yung KC, Pecht M. Physics-of-failure-based prognostics and health management for high-power white light-emitting diode lighting. IEEE Trans Device Mater Reliab 2011;11(3):407–16.

[18] Cai M, Yang D, Tian K, Chen W, Chen X, Zhang P, Fan X, Zhang G. A hybrid prediction method on luminous flux maintenance of high-power LED lamps. Appl Therm Eng 2016;95:482–90. http://dx.doi.org/10.1016/j.applthermaleng.2015.11.034.

[19] van Driel WD, Jacobs B, Watte P, Zhao X. Reliability of LED-based systems. Microelectron Reliab 2022;129:114477. http://dx.doi.org/10.1016/j.microrel.2022.114477.

[20] Ibrahim MS, Fan J, Yung WKC, Prisacaru A, van Driel W, Fan X, Zhang G. Machine learning and digital twin driven diagnostics and prognostics of light-emitting diodes. Laser Photonics Rev 2020;14(12):2000254. http://dx.doi.org/10.1002/lpor.202000254.

[21] Huang J, Golubovic DS, Koh S, Yang D, Li X, Fan X, Zhang G-Q. Degradation modeling of mid-power white-light LEDs by using Wiener process. Opt Express 2015;23 15. A966–78.

[22] Zhang Z, Si X, Hu C, Lei Y. Degradation data analysis and remaining useful life estimation: A review on Wiener-process-based methods. European J Oper Res 2018;271(3):775–96.

[23] Li J, Wang Z, Liu X, Zhang Y, Fu H, Liu C. A Wienerprocess model for accelerated degradation analysis considering measurement errors. Microelectron Reliab 2016;65:8–15.

[24] Li J, Wang Z, Zhang Y, Liu C, Fu H. A nonlinear Wienerprocess degradation model with autoregressive errors. Reliab Eng Syst Saf 2018;173:48–57.

[25] Hao H, Su C, Li C. LED lighting system reliability modeling and inference via random effects Gamma process and copula function. Int J Photoenergy 2015;2015:1–8. http://dx.doi.org/10.1155/2015/243648.

[26] Duong PLT, Park H, Raghavan N. Application of multi-output Gaussian process regression for remaining useful life prediction of light emitting diodes. Microelectron Reliab 2018;88–90:80–4.

[27] Duong PLT, Raghavan N. Prognostic health management for LED with missing data: Multi-task Gaussian process regression approach. In: 2018 prognostics and system health management conference (PHM-Chongqing). 2018, p. 1182–7.

[28] Lall P, Wei J, Sakalaukus P. Bayesian probabilistic model for life prediction and fault mode classification of solid state luminaires. In: 2014 International conference on prognostics and health management. IEEE; 2014, p. 1–10.

[29] Fan J, Yung K-C, Pecht M. Prognostics of lumen maintenance for high power white light-emitting diodes using a nonlinear filter-based approach. Reliab Eng Syst Saf 2014;123:63–72. http://dx.doi.org/10.1016/j.ress.2013.10.005.

[30] Duong PLT, Park H, Raghavan N. Application of expectation maximization and Kalman smoothing for prognosis of lumen maintenance life for light emitting diodes. Microelectron Reliab 2018;87:206–12.

[31] Tsai T-R, Lin C-W, Sung Y-L, Chou P-T, Chen C-L, Lio Y. Inference from lumen degradation data under WienerDiffusion process. IEEE Trans Reliab 2012;61(3):710–8. http://dx.doi.org/10.1109/TR.2012.2207533.

[32] Rocchetta R, Zhan Z, Di Bucchianico A. Prediction of the luminous flux degradation of light emitting diodes with an interval regressions model. In: European safety and reliability conference-ESREL 2022. 2022.

[33] Dersin P. Modeling remaining useful life dynamics in reliability engineering. CRC Press; 2023.

[34] Medina JC, Taflanidis AA. Adaptive importance sampling for optimization under uncertainty problems. Comput Methods Appl Mech Engrg 2014;279:133–62. http://dx.doi.org/10.1016/j.cma.2014.06.025.

[35] Chiao C-H, Hamada M. Robust reliability for light emitting diodes using degradation measurements. Qual Reliab Eng Int 1996;12(2):89–94.

[36] Dusmez S, Duran H, Akin B. Remaining useful lifetime estimation for thermally stressed power MOSFETs based on on-state resistance variation. IEEE Trans Ind Appl 2016;52(3):2554–63. http://dx.doi.org/10.1109/TIA.2016.2518127.

[37] Aizpurua JI, Stewart BG, McArthur SDJ, Jajware N, Kearns M, Garro U, Muxika E, Mendicute M. A diagnostics framework for underground power cables lifetime estimation under uncertainty. IEEE Trans Power Deliv 2021;36(4):2014–24. http://dx.doi.org/10.1109/TPWRD.2020.3017951.

[38] Yang X, Sun B, Wang Z, Qian C, Ren Y, Yang D, Feng Q. An alternative lifetime model for white light emitting diodes under thermal–electrical stresses. Materials 2018;11.

[39] Tan K-Z, Lee S-K, Low H-C. LED lifetime prediction under thermal-electrical stress. IEEE Trans Device Mater Reliab 2021;21(3):310–9. http://dx.doi.org/10.1109/TDMR.2021.3085579.

[40] Escobar LA, Meeker WQ. A review of accelerated test models. Statist Sci 2006;21(4):552–77. http://dx.doi.org/10.1214/088342306000000321.

[41] Luo X, Fan J, Zhang M, Qian C, Fan X, Zhang G. Degradation mechanism analysis for phosphor/silicone composites aged under high temperature and high humidity condition. In: 2017 18th international conference on electronic packaging technology (ICEPT). IEEE; 2017, p. 1331–6.

[42] Huang J, Golubović DS, Koh S, Yang D, Li X, Fan X, Zhang G. Degradation mechanisms of mid-power white-light LEDs under high-temperature–humidity conditions. IEEE Trans Device Mater Reliab 2015;15(2):220–8.

[43] Hsiao C, Pesaran MH. Random coefficient models. In: The econometrics of panel data: Fundamentals and recent developments in theory and practice. Springer; 2008, p. 185–213.

[44] Bae SJ, Kvam PH. A nonlinear random-coefficients model for degradation testing. Technometrics 2004;46(4):460–9.
[45] Sadeghi J, de Angelis M, Patelli E. Robust propagation of probability boxes by interval predictor models. Struct Saf 2020;82:101889. http://dx.doi.org/10.1016/j.strusafe.2019.101889.
[46] Sadeghi J, de Angelis M, Patelli E. Frequentist history matching with interval predictor models. Appl Math Model 2018;61:29–48. http://dx.doi.org/10.1016/j.apm.2018.04.003.
[47] Crespo L, Giesy D, Kenny S. Interval predictor models with a formal characterization of uncertainty and reliability. In: 53rd IEEE conference on decision and control. 2014, p. 5991–6.
[48] Rocchetta R, Gao Q, Petkovic M. Soft-constrained interval predictor models and epistemic reliability intervals: A new tool for uncertainty quantification with limited experimental data. Mech Syst Signal Process 2021;161:107973. http://dx.doi.org/10.1016/j.ymssp.2021.107973.
[49] Lye A, de Angelis M, Patelli E. Bayesian regression over sparse fatigue crack growth data for nuclear piping. In: Modelling in nuclear science and engineering seminar 2020. 2020.
[50] Kaplan EL, Meier P. Nonparametric estimation from incomplete observations. J Amer Statist Assoc 1958;53(282):457–81.
[51] Ferson S, Kreinovick V, Ginzburg L, Sentz F. Constructing probability boxes and Dempster-Shafer structures. Sandia National Laboratory (SNL-NM), Albuquerque, NM (United States); Sandia; 2003.
[52] Rocchetta R, Patelli E. A post-contingency power flow emulator for generalized probabilistic risks assessment of power grids. Reliab Eng Syst Saf 2020;197:106817. http://dx.doi.org/10.1016/j.ress.2020.106817.
[53] Campi M, Calafiore G, Garatti S. Interval predictor models: Identification and reliability. Automatica 2009;45(2):382–92. http://dx.doi.org/10.1016/j.automatica.2008.09.004.
[54] Campi MC, Garatti S. Wait-and-judge scenario optimization. Math Program 2018;167(1):155–89. http://dx.doi.org/10.1007/s10107-016-1056-9.
[55] Ibrahim MS, Fan J, Yung WKC, Wu Z, Sun B-J. Lumen degradation lifetime prediction for high-power white LEDs based on the Gamma process model. IEEE Photonics J 2019;11:1–16.
[56] Ibrahim MS, Jing Z, Yung WK, Fan J. Bayesian-based lifetime prediction for high-power white LEDs. Expert Syst Appl 2021;185:115627.
[57] Ibrahim MS, Fan J, Yung WK, Jing Z, Fan X, van Driel W, Zhang G. System level reliability assessment for high power light-emitting diode lamp based on a Bayesian network method. Measurement 2021;176:109191.
[58] van Driel W, Schuld M, Jacobs B, Commissaris F, van der Eyden J, Hamon B. Lumen maintenance predictions for LED packages. Microelectron Reliab 2016;62:39–44. http://dx.doi.org/10.1016/j.microrel.2016.03.018.